Understanding the mechanisms for tropical surface impacts of the quasi-biennial oscillation (QBO)

Jorge L. García-Franco[1,2], Lesley J. Gray[1,3], Scott Osprey[1,3], Robin Chadwick[4,5] and Jonathan Lin[2]

[1]Atmospheric, Oceanic and Planetary Physics, University of Oxford
[2]Lamont-Doherty Earth Observatory, Columbia University, NY
[3]National Centre for Atmospheric Science, Oxford, United Kingdom
[4]Met Office Hadley Centre, UK
[5]Global Systems Institute, Department of Mathematics, University of Exeter, Exeter, UK

Key Points:

- Nudging the zonal wind in the equatorial stratosphere affects tropical convection variability only in coupled ocean-atmosphere simulations.
- The impact of the quasi-biennial oscillation (QBO) on upper-level static stability is not sufficient to influence tropical precipitation.
- Interactions between upward wave propagation and upper-level clouds is the likely mechanism of QBO tropical teleconnections.

Corresponding author: Lesley J. Gray, `lesley.gray@physics.ox.ac.uk`

Abstract

This study evaluates the main hypotheses to explain a coupling between the quasi-biennial oscillation (QBO) in the tropical stratosphere and the tropical troposphere and surface. The impact of the QBO on tropical convection and precipitation is investigated through nudging experiments using the UK Met Office Hadley Centre Unified Model (UM). The model control simulations show robust links between the internally generated QBO and tropical precipitation and circulation. The model zonal wind in the tropical stratosphere was nudged above 90 hPa in atmosphere-only and coupled ocean-atmosphere configurations. The simulation of convection and precipitation in the atmosphere-only simulations is not statistically significantly different between the experiments with and without nudging, which may indicate that SST-convection coupling is needed for any QBO influence on the tropical lower troposphere and surface. In the coupled experiments, the precipitation and SST relationships with the QBO phase disappear when nudging is applied. Evidence from the nudging experiments shows that the QBO influence over lower stratospheric static stability is not sufficient to produce tropical surface impacts. The nudging also reduced the influence of the lower troposphere to the upper branch of the Walker circulation, irrespective of the QBO, indicating that the upper troposphere has been slightly decoupled from the surface by the nudging. These results suggest that nudging all grid-points might mute relevant feedback processes, including high cloud radiative effects and wave mean flow interactions, occurring at the tropopause level.

Plain Language Summary

The interaction between the stratosphere and the troposphere is well known to produce surface impacts in the extratropics. However, whether stratosphere-troposphere interactions affect the surface in the tropics associated with the variability of the stratospheric quasi-biennial oscillation (QBO) is yet to be determined because the observational record is too short and tropical tropospheric variability masks any potential signal of the stratosphere. In this paper, we examine hypotheses that suggest the stratospheric quasi-biennial oscillation can affect tropical deep convection to the extent of influencing tropical surface precipitation variability through targeted model experiments which prescribe the equatorial stratosphere towards observations. Our results indicate that prescribing the zonal wind in the stratosphere remove links between surface precipitation and the QBO. The weight of the evidence in our findings suggest that the impact of the QBO on the static stability at the interface of the QBO and tropical convection is not enough to produce significant effects over tropical convection and precipitation but high clouds in the tropics could play a bigger role than previously thought.

1 Introduction

The stratospheric quasi-biennial oscillation (QBO) has been linked to tropical deep convection for several decades (W. M. Gray, 1984; Giorgetta et al., 1999; Collimore et al., 2003; Liess & Geller, 2012). Observations show that the magnitude and location of tropical precipitation and several cloud properties are statistically related to the QBO phase (Liess & Geller, 2012; Tseng & Fu, 2017; L. J. Gray et al., 2018; H. Kim, Son, & Yoo, 2020; Hitchman et al., 2021; García-Franco et al., 2022; Sweeney et al., 2022). However, the extent to which the tropical troposphere and stratosphere are coupled, as well as the mechanisms that connect these two layers, remain a matter of debate (Haynes et al., 2021; Hitchman et al., 2021; Martin et al., 2021b).

Firstly, the relatively short observational record which limits our ability to detect any robust response of tropical precipitation to the QBO phase (Hu et al., 2012; García-Franco et al., 2022). The strong influence of El Niño-Southern Oscillation (ENSO) over tropical variability on interannual timescales is also a limiting factor for the attribution of anomalies in the tropics to the QBO (Liess & Geller, 2012; L. J. Gray et al., 2018; J.-H. Lee et al., 2019), especially because the ENSO-QBO relationship appears to have changed between 1960-1985 and 1985-2020 (Domeisen et al., 2019; García-Franco et al., 2022).

Secondly, there is no clear understanding of how the QBO could modulate tropical deep convection. Several hypotheses have been suggested to potentially explain a coupling of the QBO and the tropical troposphere including static stability (e.g. Nie & Sobel, 2015; Haynes et al., 2021), vertical wind shear (e.g. W. M. Gray et al., 1992), a QBO-Walker circulation feedback (Collimore et al., 2003; Hu et al., 2012; Hitchman et al., 2021; García-Franco et al., 2022) and cloud feedback hypotheses (Sakaeda et al., 2020). However, there is no clear understanding which of these hypotheses, if any, is the primary mechanism for a downward impact from the QBO on tropical convection.

The static stability hypothesis suggests that the meridional circulation driven by the descending QBO shear impacts the static stability in the region of the upper troposphere-lower stratosphere (UTLS; W. M. Gray et al., 1992; Giorgetta et al., 1999; Collimore et al., 2003; Liess & Geller, 2012; Nie & Sobel, 2015; Back et al., 2020). These studies argue that decreased UTLS static stability is found under the easterly phase (QBOE) compared to the westerly phase (QBOW), leading to enhanced convection under QBOE (Collimore et al., 2003) which could explain, e.g., the stronger convection associated with the Madden-Julian Oscillation (MJO) under QBOE conditions (Yoo & Son, 2016; Son et al., 2017; Hendon & Abhik, 2018; Back et al., 2020).

Observational and modelling results indicate that the QBO impact in the tropics is not zonally symmetric (Collimore et al., 2003; Liess & Geller, 2012; García-Franco et al., 2022). For this reason, several studies have suggested an interaction between the QBO and the Walker circulation (Liess & Geller, 2012; Hu et al., 2012; Hitchman et al., 2021). Observations show that the Walker circulation was weaker under QBOW compared to QBOE in the period of 1979-2021 (Hitchman et al., 2021; García-Franco et al., 2022) but the causal direction of this relationship remains to be well understood.

A different hypothesis, however, suggests that cloud-radiative effects (CREs) associated with the variability of tropical upper-level cirrus clouds explain the QBO-MJO link (Sun et al., 2019; Sakaeda et al., 2020; Martin et al., 2021b; Lim & Son, 2022; Lin & Emanuel, 2022). Given the importance of cirrus clouds for the radiative budget in the tropics due to their longwave CRE (Allan, 2011; Hartmann & Berry, 2017) and the role of the QBO modulating variability of clouds in the tropical tropopause layer (TTL) on interannual timescales (Liess & Geller, 2012; Davis et al., 2013; Tseng & Fu, 2017; Tegtmeier et al., 2020; Sweeney et al., 2022), the QBO could reasonably affect convection through CRE at different scales. Evidence for this hypothesis has shown that more high-cloud coverage associated with the MJO is observed during QBOE compared to QBOW (Sun et al., 2019; Sakaeda et al., 2020), suggesting that CREs associated with the QBO could be a relevant mechanism for QBO tropical teleconnections. In short, despite the growing number of hypotheses that explain a potential link between the QBO and tropical convective features, a clear mechanism remains to be determined.

Since observations and theory have not successfully identified the mechanism for QBO tropical teleconnections, several studies have turned to numerical models such as cloud-resolving models (Nie & Sobel, 2015; Martin et al., 2019; Back et al., 2020) and General Circulation Models (GCMs; J. C. K. Lee & Klingaman, 2018; H. Kim, Caron, et al., 2020; Serva et al., 2022) to identify pathways of stratospheric-tropospheric coupling. Although GCMs are more comprehensive, stratospheric and tropospheric biases have hindered the potential use of these models to tackle this problem because GCMs underestimate the amplitude of the QBO in the lowermost stratosphere (Fig. S1 and J. C. K. Lee & Klingaman, 2018; H. Kim, Caron, et al., 2020; Martin et al., 2021a). For this reason, the variability of the UTLS static stability associated with the QBO is

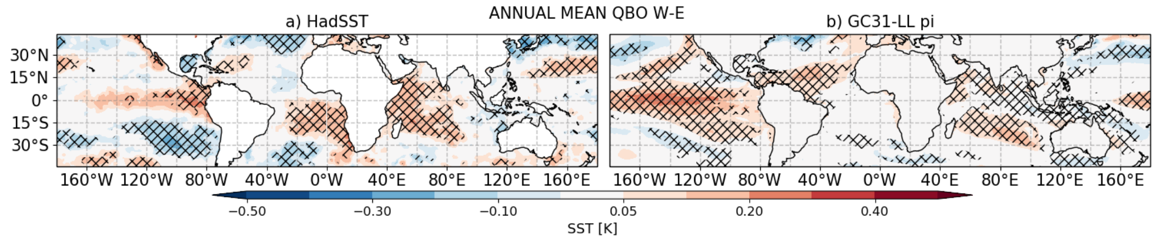

Figure 1. Annual mean SST [K] QBO W-E differences in (a) HadSST dataset and (b) the pre-industrial control simulation of the UM GC31-LL pi. Hatching denotes significance to the 95% confidence level.

lower than observed in models (Schenzinger et al., 2017; J. C. K. Lee & Klingaman, 2018; Bushell et al., 2020; Richter et al., 2020; Rao et al., 2020).

This weak amplitude bias in the QBO has been hypothesized to explain why some observed teleconnections, including the MJO-QBO relationship, are not diagnosed in GCMs (J. C. K. Lee & Klingaman, 2018; H. Kim, Caron, et al., 2020; Martin et al., 2021a). Due to these biases, several studies have performed or suggested experiments in which the model stratosphere is relaxed towards an observed or idealized state of the stratosphere, also known as nudging (e.g. Garfinkel & Hartmann, 2011; J. C. K. Lee & Klingaman, 2018; Richter et al., 2020; Martin et al., 2021a). The nudging technique can remove biases, identify causal pathways and test specific hypotheses to understand mechanisms (L. Gray et al., 2020; Haynes et al., 2021).

This study aims to understand QBO tropical teleconnections by addressing the issue of QBO model biases using relaxation experiments of the Met Office Hadley Centre (MOHC) Unified Model (UM). The UM is a state-of-the-art GCM that is able to simulate an internally generated QBO that is reasonably similar to observations, except for the weak amplitude bias in the lower stratosphere (Richter et al., 2020). In addition, nudging has previously been successfully applied in this model (Telford et al., 2008; L. Gray et al., 2020). The UM exhibits robust connections between the tropical troposphere associated with the QBO, which are described in García-Franco et al. (2022), including a sea-surface temperature (SST) signal (see Figure 1) that is similar to the observed record and El Niño events occur more frequently under QBOW compared to QBOE.

The main purpose of this study is to evaluate the effect of nudging on the representation of the QBO surface impacts in the tropics. The results of these experiments will be used to critically examine existing hypotheses suggested to explain QBO-convection links: the static stability mechanism and QBO-Walker circulation relationships, and the role of CREs. The remainder of this paper is presented as follows. Section 2 describes the nudging experiments, as well as the observations, CMIP6 and reanalysis datasets used to compare the experimental results. Section 3 presents the results of the experiments. The final section presents a discussion and conclusions arising from this study.

2 Methods and data

2.1 Observations and reanalysis

Observational data of precipitation and SSTs are used in this study. The Global Precipitation Climatology Project (GPCP) v2.3 (Adler et al., 2003) dataset is used for precipitation analyses and the HadSST v4.0 (Kennedy et al., 2019) for SST. For the remaining diagnostics, including the zonal wind and convective precipitation we use the reanalysis ERA5 from the European Centre for Medium-Range Weather Forecasts (ECMWF) (Hersbach et al., 2020) downloaded at the 0.75x0.75° resolution from `https://cds.climate.copernicus.eu/cdsapp`. In all cases the data cover the period 1979-2021.

2.2 The Met Office Unified Model

The MOHC UM uses a seamless approach modelling framework that allows the setup of simulations using various configurations; for example, various horizontal resolutions maintaining the same parametrizations and dynamical core (Walters et al., 2019). In addition to the main experimental design for nudging used in this study, which is explained in detail in the following section, the CMIP6 preindustrial control experiment from the MOHC model HadGEM3 is used for comparison. The preindustrial control experiments use constant external forcing integrated for 500 years (Menary et al., 2018). In this study we use results from the HadGEM3 GC3.1 N96 (GC31-LL) experiment.

2.3 Nudging scheme

Nudging refers to the relaxation of a model variable towards a specified state, which can be taken from reanalysis, observations or idealized states (L. Gray et al., 2020; Martin et al., 2021a). In the UM setup, three variables can be nudged: air temperature (T) and the zonal (u) and meridional (v) components of the wind; in this study we use ERA5 as the nudging data. The relaxation is applied at each grid-point, in contrast to other studies (e.g. Martin et al., 2021a) that employ a spectral model and apply the relaxation only to the zonal-mean component. Specifically, the UM uses a Newtonian relaxation technique (Telford et al., 2008; L. Gray et al., 2020) which sets the field to be nudged (F) at each time-step through the following equation:

$$\Delta F = G\Delta t(F_{ndg} - F_{model}), \tag{1}$$

where ΔF is the discrete change of F at each time-step, G is the relaxation parameter, Δt is the time-step size, F_{ndg} is the value of the field from the nudging data and F_{model} is the model value of the field at the last time-step (Telford et al., 2008).

The relaxation parameter G sets the strength of the relaxation and is linked with the relaxation timescale (τ) by $G = 1/\tau$. Previous studies (Telford et al., 2008; L. Gray et al., 2020) have shown that a 6-h relaxation time-scale is sufficient to constrain the stratosphere in the model and so the same parameter was used for the simulations of this chapter ($G = \frac{1}{6}$ h^{-1}).

Furthermore, the nudging can be performed between specified vertical levels and in selected latitude/longitude regions with *tapering*, which refers to a linear interpolation between the maximum G and zero nudging ($G = 0$). The chosen experimental design relaxes only the zonal wind (u) at all longitudes in the latitude band of 20°S-20°N, with a 10° tapering, at the model levels corresponding to 90 hPa to 4 hPa, with a vertical tapering of 4 levels, which means that full nudging was in effect only at 10°S-10°N from 70 hPa to 10 hPa. The experimental setup aims to reasonably simulate the observed variability of the zonal wind leaving the meridional component of the wind and the temperature to respond freely within the model.

2.4 Experimental design

The configuration of the UM model used for the nudging experiments is GC3.1 (version 11.4), which is the same configuration as the CMIP6 experiments (Walters et al., 2019). All the experiments, AMIP and coupled, are set up using a present-day climate configuration where all external forcings are set constant to those of the year 2000. The atmospheric horizontal resolution is N96 (1.875°x1.25°) for our experiments. A summary of all the experiments is given in Table 1.

The atmosphere-only (AMIP) experiments were conducted for 32 years (1981-2012) using prescribed SST and sea-ice boundary conditions for the period 1981-2012, using the data provided as part of the CMIP6 AMIP forcing setup. Three sets of AMIP experiments were run: Con-

Table 1. Experimental setup indicating the model configuration, the period, number of ensemble members (Ens.) and relaxation details.

Name	Configuration	Period	Ens.	Nudging
AMIP	Atmosphere-only	1981-2012	3	ERA5.
AMIP-Control	Atmosphere-only	1981-2012	3	No nudging
AMIP-Shifted	Atmosphere-only	1981-2012	3	ERA5 Relaxation shifted -1 year.
Coupled Nudged	Coupled ocean-atmosphere	1981-2015	6	ERA5.
Coupled Control	Coupled ocean-atmosphere	1981-2015	6	No nudging

trol, Nudged and Shifted. In the control experiment, the model stratosphere was free to evolve. In the Nudged experiment, the equatorial zonal wind was nudged, as described in the previous section, with the nudging wind data matching the corresponding SST data.

In addition, we performed another type of atmosphere-only experiment, the Shifted experiment. In the normal AMIP Nudged experiment, the SST driving data corresponds to the same year as the nudged zonal wind in the equatorial stratosphere. In the Shifted experiment, the nudging data was shifted with a -1 year lag from the SSTs, e.g., the model year 1997 was run using 1997 SSTs but zonal winds in the stratosphere corresponding to 1996. An alternative approach would be to *shuffle* the SSTs so that each year is run with randomly selected SSTs. However, since we are performing multi-year simulations shuffling has associated issues of how to join the randomly-selected SSTs at the year-boundary to form a coherent multi-year SST time-series. To avoid this issue we decided to simply shift the zonal wind nudging data by one year so the QBO phase and SSTs were not aligned.

For the coupled ocean-atmosphere experiments, a control and a nudged ensemble of 6 members were run for 35 years (1981-2015 model years). The coupled experiments use an oceanic resolution of 0.25° (ORCA025) using the NEMO model (Storkey et al., 2018). Each ensemble member was initialized from different ocean/atmosphere initial conditions, in order to decrease the role that internal variability may have on these simulations by averaging out the ensemble. Specifically, the coupled ocean-atmosphere configuration was initialized using oceanic conditions from a 100-yr simulation of the same model configuration that were found 10 years apart from each other.

2.5 Indices and methods

ENSO is measured through the standard Oceanic Niño Index, i.e., the time-series of area-averaged SSTs in the Niño 3.4 region (hereafter EN3.4 Trenberth, 1997) and a 5-month running mean using a 0.5 K threshold to define positive or negative events. The QBO index is defined using the equatorially-averaged [10S-10N] zonal winds at the 70 hPa level and a ± 2 m s^{-1} threshold to define W and E phases. A measure of the zonal gradient of convective activity in the Indian Ocean is used as a proxy of the Indian Ocean Dipole (IOD), as in García-Franco et al. (2022). Composite and regression analysis are used to evaluate the differences amongst experiments, as in García-Franco et al. (2022). Statistical significance in observations and individual ensemble members is diagnosed using a bootstrapping method with replacement, whereas for all ensemble-mean differences, given their relative larger sample size, standard two-sided t-tests are used.

3 Results

Figure 2 demonstrates that nudging increases the UTLS temperature and zonal wind variability associated with the QBO. The comparison of the QBO W-E difference between the nudged experiments, ERA5, the 500-yr CMIP6 GC31-LL simulation, and the control experiments shows that the nudged experiments closely resemble the results from ERA5 whereas the control experiments exhibit a much weaker signal. In the tropical UTLS region, the nudged experiments show a wider and stronger QBO signal than the control experiments which demonstrates that these experiments are suitable to explore the processes that relate the QBO with the tropical surface. The control-nudged difference plots (Fig. S2) illustrate that the warm anomalies near the equatorial tropopause between 70-90 hPa are up to 1.5 K larger in the nudged experiments.

Since the nudging technique has removed the weak QBO amplitude bias in the lower stratosphere, we now analyse tropical teleconnections in these experiments. First, results from the atmosphere-only experiments are analysed, followed by the analysis of the coupled experiments. The final section investigates the mechanisms that could explain the differences between nudged and control experiments.

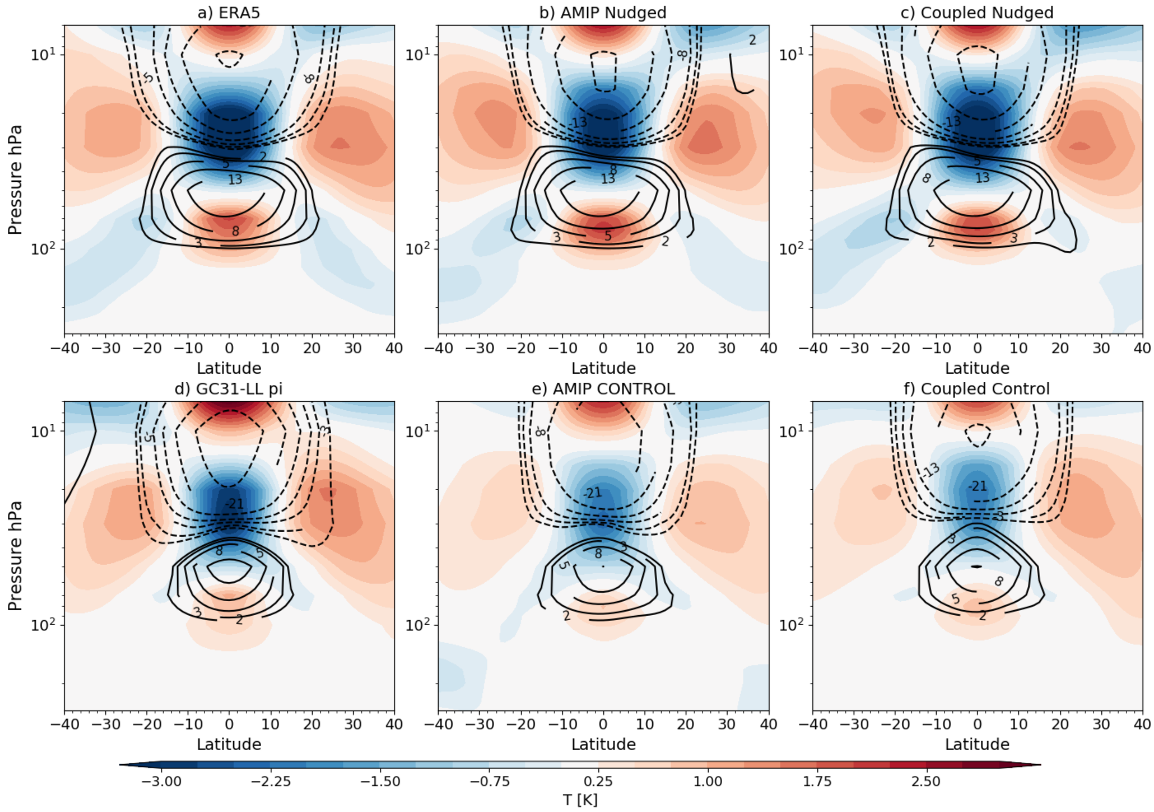

Figure 2. Latitude-height plot of the zonal-mean temperature (shading) zonal wind (contours in m s^{-1}) QBO W-E differences in (a) ERA5, the nudged simulations in (b) AMIP and (c) coupled configurations and (d) GC3 N96-pi from CMIP6, the control simulations with no nudging in an (e) AMIP and (f) coupled configurations

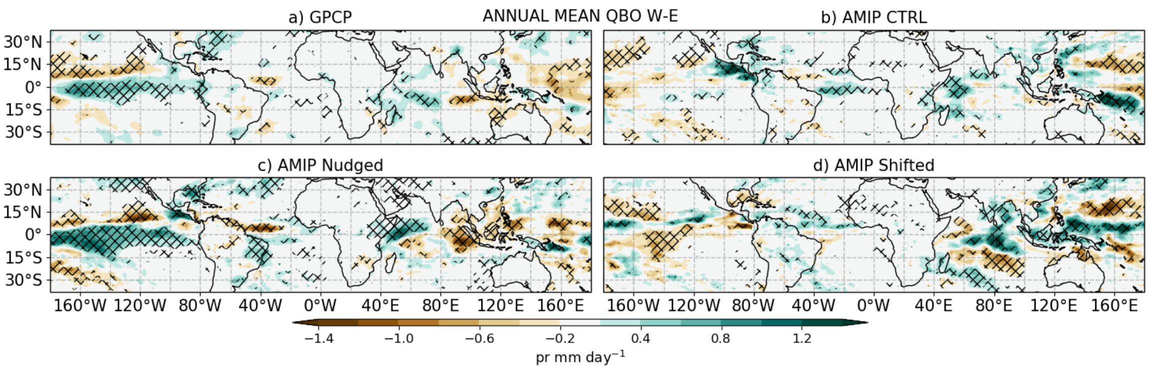

Figure 3. Annual-mean precipitation response (QBO W-E) in (a) GPCP, and atmosphere-only experiments: (b) AMIP CTRL, (c) AMIP Nudged and (d) AMIP Shifted.

3.1 Atmosphere-only experiments

This section shows the results of the atmosphere-only experiments: AMIP Nudged, AMIP Control and AMIP Shifted (in which the imposed winds have been shifted by a year so there is an out-of-phase relaxation of the winds with respect to the SSTs), compared to observations (1981-2012). The annual-mean difference of precipitation between QBOW and E phases from the three experiments are compared with GPCP differences in Fig. 3. The AMIP Nudged ensemble-mean matches closely the results of GPCP, characterised by an El Niño pattern in the Pacific Ocean, a weaker Atlantic ITCZ and a zonal gradient of precipitation in the Indian Ocean during QBOW compared to QBOE.

In contrast, the differences in the AMIP Control and the AMIP Shifted experiments show little similarity to the observed response, a similar result is found for seasonal-mean composite differences (see e.g. Fig S3). The fact that the QBO response is different in the three types of AMIP experiments suggests that the underlying SSTs, and not the QBO winds, are responsible for these differences. However, it may still be the case that tropical convection is sensitive to the QBO phase in these simulations and this effect is hidden by the strong effect of SST forcing.

Time-series of multiple diagnostics averaged at equatorial latitudes and in the EN3.4 regions are shown in Figure 4. The tropical mean outgoing longwave radiation (OLR) and precipitation is not significantly affected by the nudging, suggesting that convective activity is independent from the state of the QBO at 70 hPa. The correlation coefficients of precipitation and OLR with respect to observations (a-b) are indistinguishable between experiments, both for the tropics-wide (a, c) and for the EN3.4 region (b, d).

The timeseries of the equatorial zonal mean zonal wind at 70 hPa (U_{70}; Fig. 4e) shows a correlation between ERA5 and the Nudged experiment, as expected. In contrast, the correlation of ERA5 with AMIP CTRL is virtually zero, because the ensemble-mean zonal wind of the CTRL collapses to near zero values. The Shifted experiment shows a negative and high correlation (0.65) with ERA5, which is not surprising, since the SSTs have been shifted by one year i.e. approximately half a QBO cycle.

The timeseries of the near-tropopause temperature (T_{100}; Fig. 4g-h) shows that the Nudged ensemble is correlated with ERA5 in the tropical mean. This correlation increases for the EN3.4 region in all the experiments such that the three simulations are well correlated with ERA5, although the Shifted experiment shows the lowest correlation. These results suggest the near-tropopause temperature is controlled by the QBO in the zonal-mean but by local SSTs at regional scales.
In short, this section shows that in atmosphere-only experiments the nudging produces the ex-

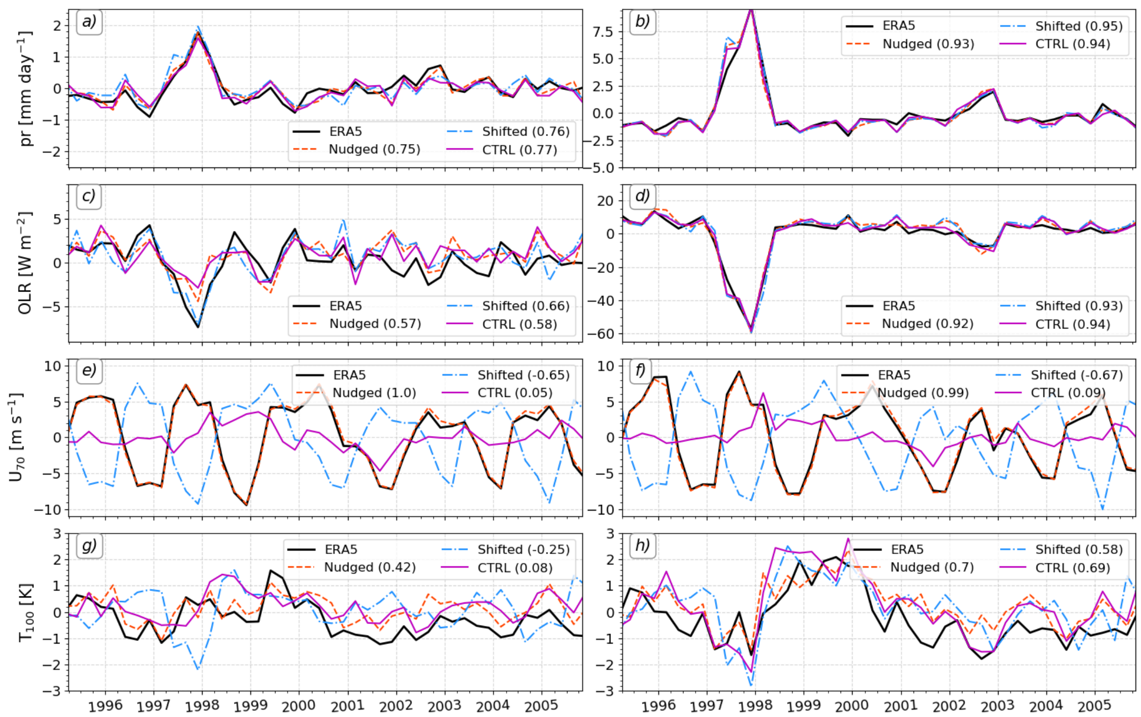

Figure 4. Time-series in the atmosphere-only experiments of (a, b) precipitation, (c, d) outgoing long-wave radiation (OLR), (e, f) zonal wind at 70 hPa (U_{70}) and (g, h) air temperature at 100 hPa. The timeseries are shown for quantities averaged over the (left) zonal-mean equatorial [5°S-5°N] and (right) EN3.4 regions. For each AMIP experiment the Pearson correlation coefficient between the experiment and ERA5 is shown in the legend. Note that the model year refers to the SST years as described in section 22.4.

pected impacts in U_{70} and the zonal-mean T_{100}, however, the nudging appears to have no made impact on the simulation of precipitation and OLR.

3.2 Coupled experiments

This section analyses the coupled ocean-atmosphere experiments, labelled as the Coupled Nudged and the Coupled Control simulations, which consist of 6 ensemble members (see section 22.4). The SST response is first examined through the annual mean QBO W-E ensemble-mean difference in tropical SSTs of the coupled control experiments (Fig 5a-b) which compares reasonably well with the results from HadSST and GC3 LL-pi (Fig. 1). This response is characterized by warmer SSTs (+0.2-0.3K) during QBOW than during QBOE in the deep tropics and generally cooler subtropical oceans. However, for the Coupled Nudged ensemble-mean, the tropi-

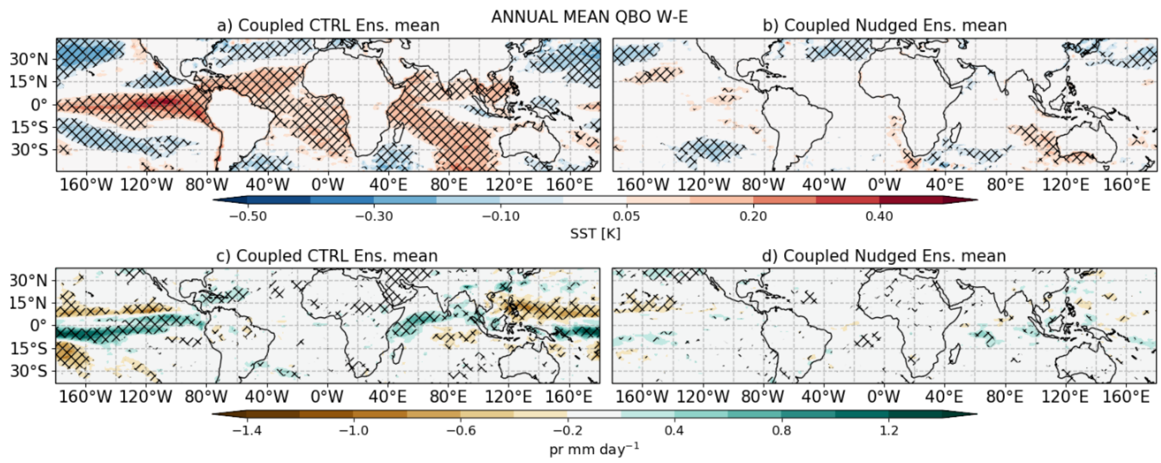

Figure 5. As in Fig, 1 but for results of the (a, c) Coupled Control and (b, d) Coupled Nudged ensemble-mean (a, b) SST [K] and (c, d) precipitation [mm day^{-1}].

cal response is essentially zero, although some sparse regions showing slight cooling (W-E) can be observed in the subtropics. This means that the nudging has affected the physical mechanism behind the robust statistical relationship between the tropical SSTs and the QBO phase in the UM (García-Franco et al., 2022).

The QBO W-E differences in each of the 6 ensemble members in the Control and Nudged experiments (Fig. S4) show that the weak response in the ensemble-mean of the nudging experiments is the result of very different responses from each ensemble member. These individual responses cancel out to a large extent. In contrast, most of the control ensemble members exhibit a warming signal in the equatorial oceans, leading to the statistically significant response seen in the ensemble-mean.

The precipitation response (Fig. 5c-d) follows closely the SST patterns. The robust relationship between the QBO and tropical precipitation in the UK UM (García-Franco et al., 2022) is also observed in the Control experiment characterized by shifts of the ITCZ in the Pacific and Atlantic sectors and a wetter western Indian Ocean. This relationship is, however, removed, when the nudging is applied as the nudged ensemble-mean is virtually zero across the tropics, which is also due to the cancelling effect of different responses in individual ensemble members (Fig. S5).

One key result from García-Franco et al. (2022) was a robust relationship between the QBO and the IOD during boreal fall. Figure 6 shows that this relationship is also robust in the Con-

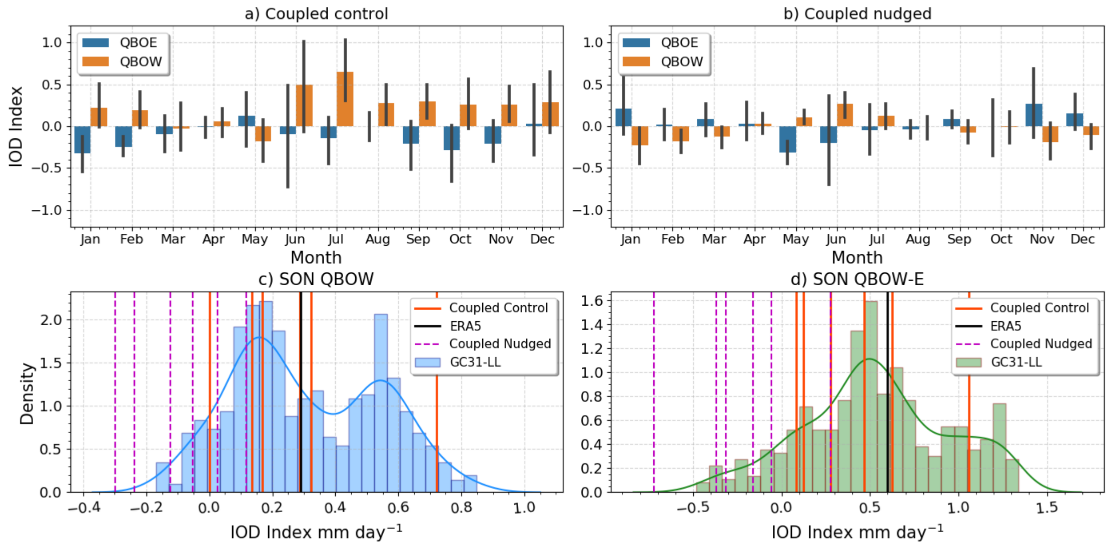

Figure 6. (a, b) Monthly-mean convective precipitation IOD index [mm day^{-1}] in coupled (a) control and (b) nudged ensemble-means separated by QBO phase; the error bars indicate ensemble spread. (c, d) Probability density functions (PDFs) of the IOD convective precipitation index for (c) the mean SON during QBOW months and (d) the SON difference between QBO W-E. The PDF is obtained by bootstrapping the 500 yr simulation of the GC31-LL 42-yr periods and obtaining the averages and differences in each sub-sample. The mean values for the Coupled Control and Nudged experiments, as well as for ERA5 are shown as vertical lines.

trol experiments of this configuration but not in the Coupled Nudged experiments. A probability density function (PDF) of QBO W-E in the IOD index was constructed using 35-yr chunks of the pre-industrial control experiment GC31-LL to sample internal variability within the model. The difference in the IOD index per QBO phase for individual ensemble members from the Control and Nudged experiments is plotted together with the GC31-LL PDF (Fig. 6c-d) to examine the likelihood that the results from the Nudged experiments happen by chance.

The results in Fig. 6c-d strongly suggest that the influence on the IOD is removed when nudging is applied given that some ensemble Nudged members show differences that are outside of the 99% range of the PDF whereas all the Control experiments show results that fall close to the median of the GC31-LL PDF. The results for the EN3.4 index are very similar (Supplementary Fig. S6) confirming the ENSO-QBO relationship has been removed by the nudging.

This section shows that the coupled control experiments in our configuration broadly reproduce those of García-Franco et al. (2022), i.e., wamer SSTs and wetter conditions in the deep tropics in QBOW compared to QBOE as well as statistical links between the QBO and ENSO and the IOD. However, nudging has significantly affected the relationships between the QBO and the tropical troposphere. Several plausible explanations, including the possibility that the statistical relationships diagnosed by García-Franco et al. (2022) are simply due to an upward effect from the troposphere to the stratosphere, are discussed in the final section. The following section evaluates three hypotheses using these experiments.

3.3 Mechanisms

The main mechanisms suggested by the literature to possibly explain a role for the QBO in modulating aspects of tropical convection are the static stability, QBO-Walker circulation and high-cloud effects. This section aims to evaluate these hypotheses through a comparison of the coupled nudged and Control experiments.

3.3.1 The static stability hypothesis

The effect of the QBO over the tropical UTLS temperature structure has been well documented (Tegtmeier et al., 2020; Martin et al., 2021c) and is, arguably, the most frequently suggested mechanism that relates tropical convection variability to the QBO (Collimore et al., 2003; Liess & Geller, 2012; Hu et al., 2012; Nie & Sobel, 2015; J. C. K. Lee & Klingaman, 2018; Hitchman et al., 2021). The UTLS static stability is defined here by the temperature difference (ΔT) between 150 and 70 hPa, so that negative values indicate decreased stability. Other definitions of ΔT such as the temperature difference between 250 hPa and 70 hPa, as well as using the 100 hPa temperature filed as a proxy yield similar results to our definition.

Figure 7 shows the QBO (W-E) signal in ΔT and convective precipitation. The spatial distribution of the ΔT differences is relatively zonally symmetric, although for ERA5 and the nudged experiments ΔT maximizes in the Eastern Pacific. The magnitude of the QBO-related variability in ΔT is doubled by the nudging in the deep tropics compared to the control experiments, however the precipitation response is not increased in the nudged experiment. The precipitation response to the QBO in models and observations is, firstly, not zonally symmetric and secondly, not collocated with the largest influence of the QBO signal on the static stability differences.

The relationship between the UTLS static stability and tropical precipitation is investigated in more detail in Figure 8. This figure shows several scatter plots of the spatial and temporal relationship between the static stability and precipitation in both reanalysis and our model sim-

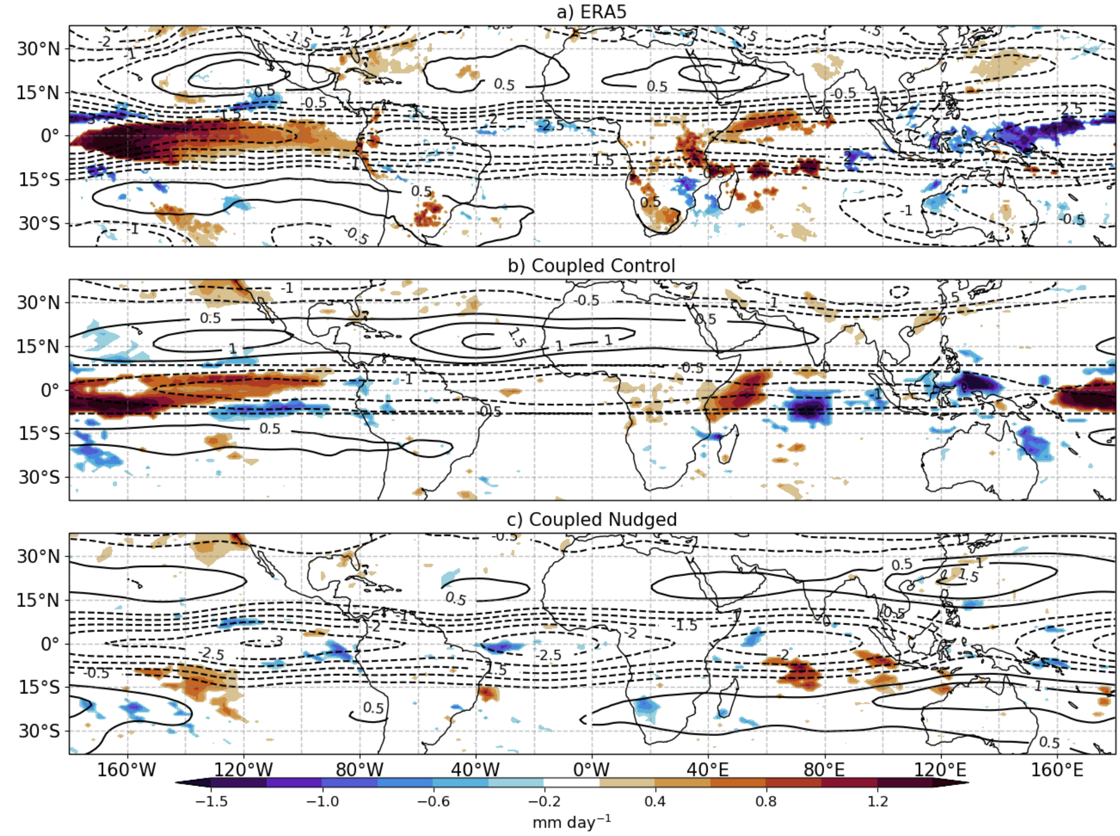

Figure 7. Convective precipitation (shading) and UTLS static stability (ΔT contours in [K]) DJF composite differences (QBO W-E) in (a) ERA5 and the ensemble-mean Coupled (b) Control and (c) Nudged experiments. Only statistically significant differences to the 95% confidence level are plotted.

ulations. First, Figure 8a shows the scatter plot of the monthly-averaged ΔT versus Δpr in the equatorial Western Pacific; such that each points represents a month in ERA5. Therefore, this figure shows that these two variables have a very weak temporal correlation. In other words, in ERA5, the temporal variability of the UTLS static stability is not related to precipitation variability in the West Pacific warm pool. The sign of the correlation coefficient (weak in any case) reverses between QBOW months and QBOE months. Similar results are found for the simulations (not shown).

Next, Figure 8b shows a scatterplot of the annual mean QBO W-E differences of ΔT versus Δpr at each grid-point in the Coupled nudged and Coupled Control experiments. The magnitude of the negative ΔT differences is higher in the nudged experiments than in the control whereas the spread of the precipitation differences is higher in the control. This figure illustrates that the nudging increases the spread of the ΔT differences but not of precipitation. Moreover, in the con-

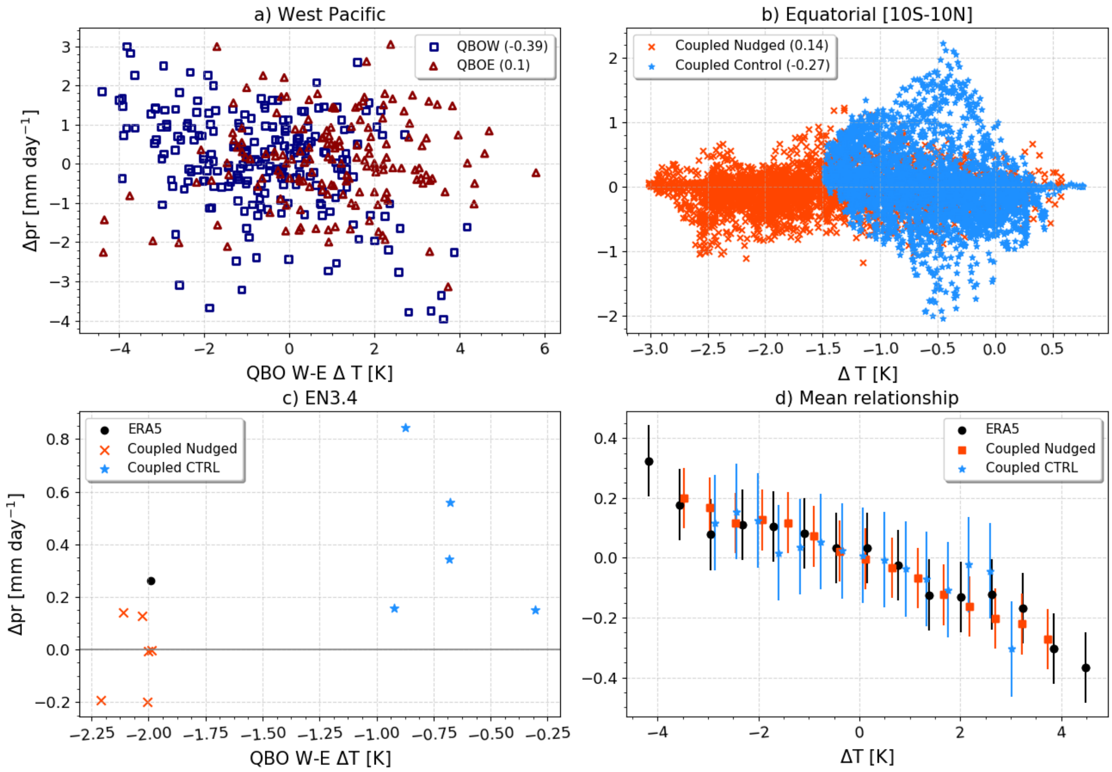

Figure 8. a) Scatter plot of deseasonalized convective precipitation [Δpr mm d^{-1}] versus UTLS static stability [ΔT K] anomalies for the western equatorial Pacific [0-10N,120-160E] in ERA5. Each data-point represents a month in the 1979-2021 period. b) As in a) but for the DJF ensemble-mean QBO W-E differences in the equatorial latitudes [10S-10N] in the simulations, so each dot represents a grid-point. c) Scatter plot of the annual-mean QBO W-E differences in Δ pr versus ΔT in the EN3.4 region for each ensemble member of the simulations and ERA5. d) Mean relationship of Δ pr versus ΔT computed by binning ΔT in all the grid-points at all times and computing the corresponding mean Δ pr.

trol experiments, both positive and negative precipitation differences are found for similar ranges of ΔT differences. The existence of both positive and negative differences in Δpr for similar values of ΔT in the control indicates that there is no unique longitudinally coherent or zonally symmetric impact of the QBO. Additionally, this plot suggests that the magnitude of the precipitation differences are not explained by ΔT differences.

Then, Figure 8c shows how annual mean QBO W-E differences in ΔT are related to Δpr in the Niño3.4 region for each ensemble member of the control and nudged experiments. All the coupled control ensembles show a positive precipitation difference (W-E) of up to 0.85 mm day^{-1}, even though the static stability difference (W-E) is half as strong compared to the nudged experiments. The nudged ensemble members, in contrast, simulate both positive and negative precipitation responses close to 0, indicative of no statistical relationship between ENSO and the QBO in these experiments.

Finally, Figure 8d analyses the average relationship between ΔT and Δpr. In this plot, all the monthly-mean anomalies of convective precipitation and absolute values of ΔT have been composited using all the grid-points at equatorial latitudes [10°S-10°N] for all the months in each simulation. This procedure pairs Δpr and ΔT taken at the same time and space coordinates. From this composite, the average Δpr anomalies were computed for equally-separated bins of ΔT (starting at the 1th pecentile and up to the 99th percentile). In this plot, the variability of ΔT is not necessarily associated with the QBO but the purpose of this plot is investigate whether precipitation anomalies are related to the upper-level temperature structure more generally.

Therefore, Figure 8d shows the average precipitation anomaly for each ΔT bin. The mean relationship across the different datasets appears to be of a weak negative relationship which becomes significant for high absolute values of ΔT characterized by higher static stability associated with less precipitation and decreased UTLS static stability associated with more precipitation. This result would support the main assumption of the static stability mechanism, i.e., that decreased upper level static stability associated with the QBO leads to more precipitation. This Figure also confirms that the nudging has increased ΔT variability but the nudging has only increased precipitation variability only for negative ΔT values.

The implication from these results is that nudging has increased ΔT variability and indeed UTLS static stability is linked to precipitation, however, the time-mean composite differences, shown in the previous section, suggest that these local-scale ΔT impacts are not enough to simulate a time-mean significant signal on surface precipitation. In other words, this section presents evidence that in the UM and ERA5, QBO-related changes to static stability are not a sufficient factor to modulate tropical convection.

3.3.2 The Walker circulation

Several studies have suggested a link between the QBO and the Walker circulation (Liess & Geller, 2012; Hitchman et al., 2021; García-Franco et al., 2022): specifically, in the UM the Walker circulation is weaker under QBOW than under QBOE. Figure 9 shows the impact of nudging on the mean state and QBO-ENSO related variability of the Walker circulation. The biases in the mean-state of the Walker circulation are large in the control experiment, with differences

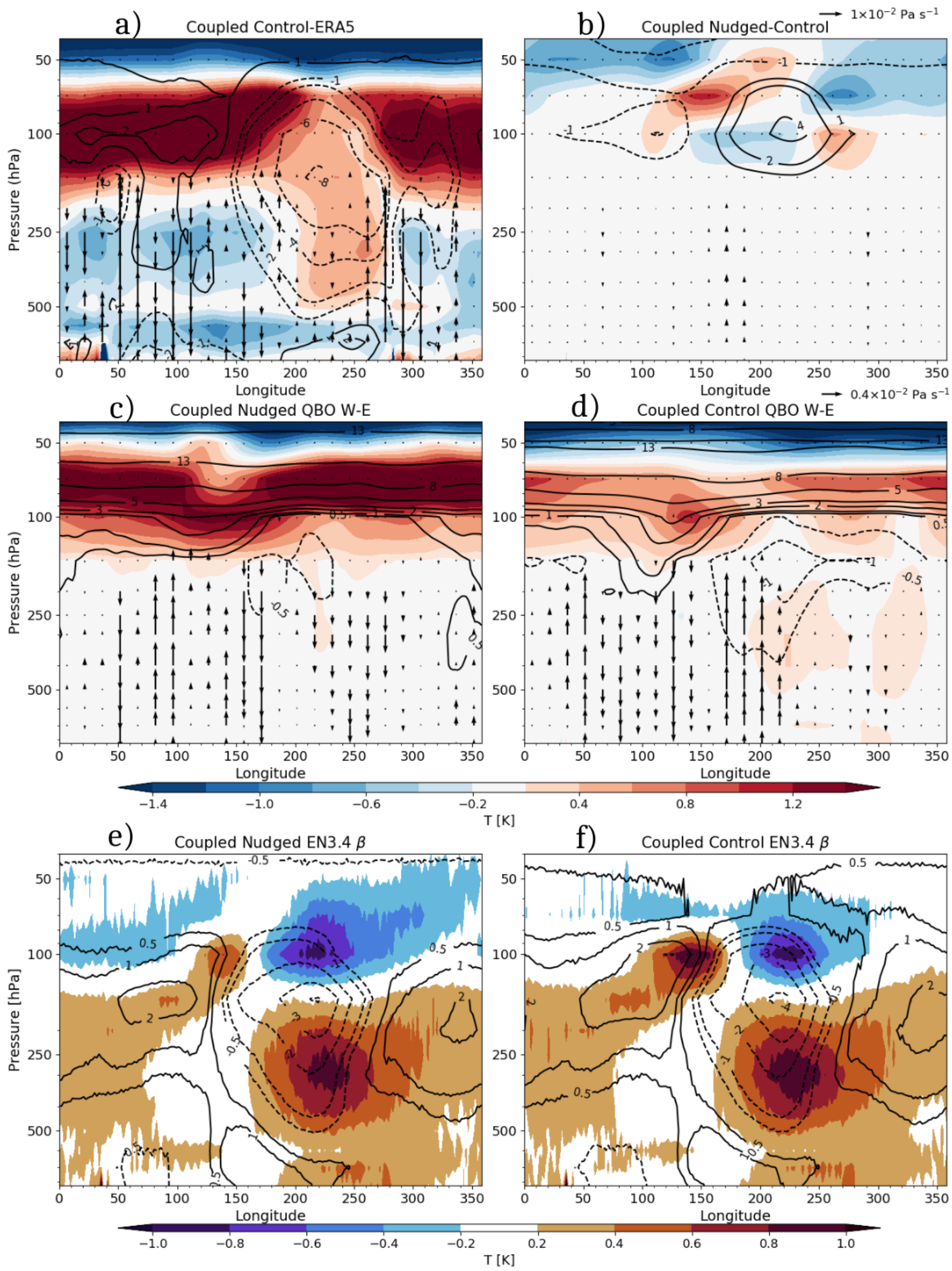

Figure 9. (a) Mean biases, diagnosed as differences between control ensemble-mean and ERA5, in the Walker circulation, (equatorial averages [10S-10N]) diagnosed from the zonal mean temperature (K in shading), zonal wind (contours in m s^{-1}) and vertical velocity (vectors in Pa s^{-1}). (b) shows the differences between nudged and Control coupled experiments. (c-d) show the QBO W-E differences for the (c) nudged and (d) Control ensemble-mean. (c-d) is as in (a-b) except that the (c-d) vector key is different than for (a-b). (e-f) show the results of the regression coefficients (β) between the zonal wind (contours) and the air temperature (shading) fields with the EN3.4 index.

of up to 6 m s^{-1} and 1.5 K compared to ERA5 (Fig. 9a). However, nudging improves some of the zonal wind biases (b), especially in the Pacific Ocean, while also producing an impact on UTLS temperature biases (≈0.5 K).

The QBO-related Walker circulation variability appears to be affected by the nudging. In the upper troposphere, the QBO impact on the zonal wind and vertical velocities is different for nudged and control experiments (c versus d). This difference is more obvious in the Indian Ocean sector where the control experiments suggest that the W-E response is characterized by anomalous ascent in the western sector and descent in the eastern sector, yet the nudged response is the opposite.

Regression analysis was used to investigate the interaction of ENSO, the QBO and the Walker circulation, as in García-Franco et al. (2022). Figures 9e-f suggest that not only are the mean-state and the QBO relationships affected but the linear relationship between ENSO and the upper branch of the Walker circulation is weakened when the nudging was applied (see e.g. 150E at 100 hPa where the temperature signal is twice as large in the control experiment). Note, however, that the lower tropospheric ENSO signal remains unchanged.

These results suggest that the effect from ENSO on to the UTLS temperature has been weakened by the nudging which suggests that the nudging may have overly constrained the upper-branch of the Walker circulation. Feedback processes between convection and the UTLS temperature may have been reduced in strength and the temperature field, constrained through thermal wind balance, which are perhaps related to the nature of the nudging conducted in this study (see section 4 for a more detailed discussion on this possibility).

3.3.3 The CRE hypothesis

High cirrus CREs are a key aspect of tropical climate (Hartmann & Berry, 2017; Byrne & Zanna, 2020) such that recent studies have suggested mechanisms through which CREs explain the observed MJO-QBO connection (Sun et al., 2019; Lin & Emanuel, 2022; Lim & Son, 2022). This section uses model diagnostics that are relevant to this hypothesis such such as outgoing longwave radiation (OLR), cloud top pressure (CTP), high cloud fraction (HCF %) and ice total content (QCF) to better understand the differences between control and nudged experiments.

The annual mean difference in HCF and QCF associated with the QBO phase (Fig. 10) shows that the relationship between high clouds and the QBO is different in nudged versus con-

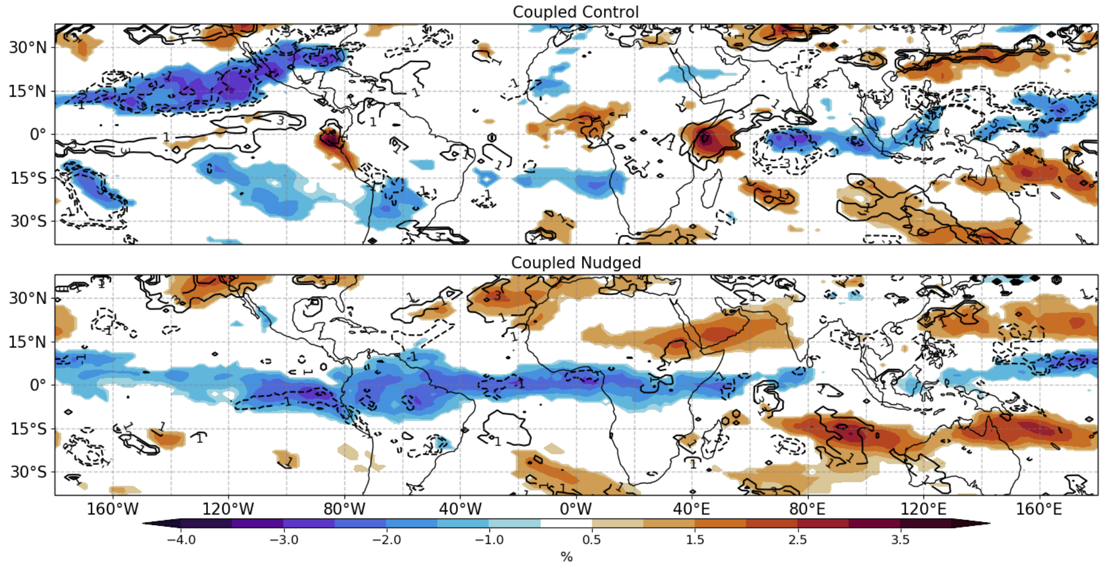

Figure 10. Annual mean differences (QBO W-E during ENSO neutral periods) in high cloud fraction [shading in %] and ice cloud water content [contours in 10^{-2} kg m^{-2}] for Coupled Control and nudged experiments. Only statistically significant (95% confidence level) differences are plotted.

trol coupled experiments. In the nudged experiments, the QBO signal is much more zonally symmetric, characterized by reduced HCF and QCF at equatorial regions under QBOW compared to QBOE, in agreement with previous observational and modelling studies (Sun et al., 2019; Sakaeda et al., 2020; Sweeney et al., 2022). In contrast, the differences (W-E) in the free-running control simulations show a zonally asymmetric response, e.g., with a dipole of positive and negative anomalies in the Indian Ocean.

Figure 11 shows the zonal-mean differences (QBO W-E) in convective precipitation and high cloud diagnostics. First, the control experiments show a dipole response of convective precipitation dipole response in the Indian Ocean, first reported by García-Franco et al. (2022), which is also observed in OLR, HCF and QCF. In the control experiments, precipitation differences are strongly anti-correlated with OLR, as expected, and positively correlated with CTP, HCF and QCF, which illustrates that high cloud occurrence is linked to convective precipitation. However, the nudged experiments do not exhibit such clear relationships. Instead, the nudged experiments show a zonally symmetric decrease of HCF under QBOW compared to QBOE. This could suggest that the without dynamical feedbacks, the QBO impact is to decrease HCF at equatorial latitudes.

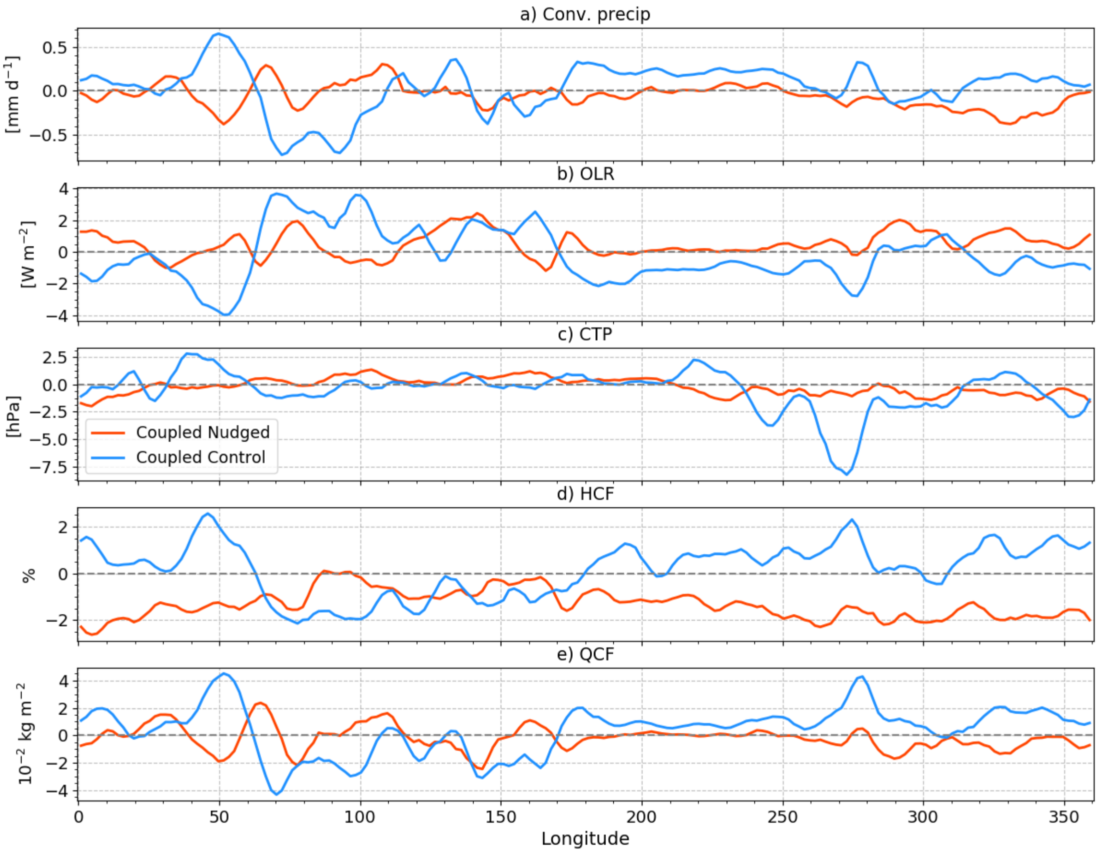

Figure 11. Zonal-mean equatorially averaged [10S-10N] annual-mean differences QBO W-E (during neutral ENSO conditions only) of (a) convective precipitation [mm day^{-1}], (b) OLR [W m^{-2}], (c) cloud top pressure [Pa], (d) high-cloud fraction [%] and (e) ice total content [10^{-2} kg m^{-2}].

In short, this section shows that when the stratosphere is nudged fewer high clouds are found under QBOW compared to QBOE at equatorial latitudes. In contrast, the control experiments show zonally asymmetric signals, particularly in the Indian Ocean, which closely follow precipitation and OLR anomalies. These results suggest that the interaction between high clouds and the QBO phase has been modified by the nudging. Despite exhibiting robust zonally symmetric anomalies in HCF, the nudged experiments do not show spatially coherent or robust convective precipitation differences. This result could suggest that changes to high cloud fraction or ice content alone are not sufficient for a significant precipitation response.

4 Discussion and conclusions

A set of nudging experiments performed with the MOHC UM was used to investigate three existing hypotheses that could explain links between the QBO and tropical convection and precipitation. By nudging the zonal wind in the equatorial stratosphere towards ERA5, the UM realistically reproduces the observed QBO-related variability in the zonal wind and temperature in the UTLS region. The nudging thus removed the weak QBO amplitude bias in the lower stratosphere which could modify or weaken QBO tropical surface impacts in GCMs (J. C. K. Lee & Klingaman, 2018; H. Kim, Caron, et al., 2020; Martin et al., 2021a).

The analysis of the atmosphere-only experiments has shown that the zonal wind in the equatorial stratosphere, either nudged or free-running, makes little difference to the simulation of precipitation in the UM with prescribed SSTs as boundary conditions. This result implies that any process that links the QBO to the tropical circulation within the model, such as those diagnosed in García-Franco et al. (2022), requires SSTs to play an active role, either driving the relationship or through SST-QBO feedbacks.

The role of SST feedbacks for the QBO mechanism was investigated using coupled ocean-atmosphere experiments. In the control experiments, the SSTs over tropical oceans were found to be warmer under QBOW than under QBOE, in agreement with García-Franco et al. (2022). Precipitation patterns in these experiments follow the SSTs with wetter conditions over equatorial oceans under QBOW compared to QBOE. However, in the nudged ensemble-mean, both SST and precipitation differences were null or close to zero in equatorial regions, meaning that the relationship between the QBO and the tropical surface in the control experiments was muted by the nudging. A closer inspection of other relationships between the QBO and the IOD and ENSO (García-Franco et al., 2022), confirmed that the nudging has notably modified, and in some cases removed, the QBO signal at the tropical surface.

One possible explanation for these results is that the simulated QBO-tropical teleconnections are the result of a bottom-up process which is broken when the stratosphere is nudged towards a specified state. Since the QBO is tightly coupled to the interaction between convectively triggered waves and the stratospheric mean flow (Baldwin et al., 2001; Y.-H. Kim & Chun, 2015; Geller et al., 2016; Garfinkel et al., 2022), the QBO is modulated by tropical variability such as ENSO events (Schirber, 2015; Serva et al., 2020). Therefore, one could reasonably suspect that the difference between the control and the nudged experiments is simply that waves propagating from the tropical troposphere cannot propagate to the nudged layer in the nudged experiments.

However, previous studies have found no evidence for an impact from ENSO on to the QBO amplitude and descent rates in the UM (Serva et al., 2020; García-Franco et al., 2022). While tropical waves propagated from the troposphere to the stratosphere are a main control of the QBO characteristics, the impact of upward tropical wave propagation is subtle and does not instantaneously change the zonal mean wind at 70 hPa (which is our index). This means that the ENSO-QBO relationship in the UM model remains to be explained.

Another possibility is that feedbacks that are responsible for the relationships simulated in the control simulations were removed by the nudging. This possibility was investigated using elements from three hypotheses that could explain QBO teleconnections in the tropics: the static stability, the Walker circulation and high cloud feedbacks. The static stability hypothesis suggests that the UTLS temperature structure, affected by the QBO on interannual timescales, can modify the strength of convection such that decreased UTLS static stability under QBOE increases convection and precipitation compared to QBOW (Collimore et al., 2003; Liess & Geller, 2012).

However, this study shows that the magnitude and sign of the UTLS static stability variability associated with the QBO (Figs. 7 and 8) have no robust relationship with precipitation variability in the deep tropics in the UM. First, the QBO signal in UTLS static stability was found to be zonally symmetric but the QBO signal in precipitation was highly asymmetric. Second, the nudged experiments more than doubled the UTLS static stability variability associated with the QBO, yet the precipitation response to the QBO phase was muted when the nudging was applied, Nevertheless, variability in the UTLS static stability is indeed positively correlated to precipitation variability over tropical oceans (Fig. 8d). The implication from this result is that QBO-related variability in UTLS static stability is not a sufficient process to explain the link between the QBO and tropical convection and other processes amplify or overwhelm the influence of the static stability.

A second hypothesis argues that the Walker circulation strength and location is affected by the QBO, which could explain why the precipitation response in the tropics is zonally asymmetric (Hitchman et al., 2021; García-Franco et al., 2022). The coupled experiments showed that the nudging significantly affected the mean-state and variability of the upper branch of the Walker circulation in the Pacific and maritime continent. A weakening of the Walker circulation under QBOW compared to QBOE is diagnosed in observations, the control experiments and other versions of the UM model (Hitchman et al., 2021; García-Franco et al., 2022). However, the QBO-Walker circulation relationship was weakened when the nudging was applied to the model. In fact, the Indian Ocean response even reversed sign relative to the control. One possible explanation is that the nudging has overly constrained the upper branch of the Walker circulation, removing mean-state biases and, to some extent, the influence from the SSTs on to the 200-100 hPa temperature and wind fields (Fig. 9e-f). This result could mean that the Walker circulation plays a role in amplifying local-scale effects of the QBO in a feedback process which was modified by the nudging. used, including cloud fraction and ice cloud content, an Finally, a CRE hypothesis has been suggested recently which argues that cirrus clouds play an important role in QBO tropical teleconnections (Sun et al., 2019; Sakaeda et al., 2020; Lin & Emanuel, 2022). This CRE hypothesis could operate at the large-scale, if the QBO modifies the mean-state of clouds in the TTL region (Tseng & Fu, 2017; Sweeney et al., 2022) but also at the convective scale if strength of ascent and vertical advection of water vapour is modified by the QBO (Nie & Sobel, 2015; Sakaeda et al., 2020).

To investigate this hypothesis, several diagnostics for high clouds were shown to be positively correlated with precipitation changes in the control experiments. In the nudged experiments, a robust decreased fraction of high clouds under QBOW compared to QBOE is diagnosed across equatorial regions, which agrees with some observational and modelling evidence (Sun et al., 2019; Sakaeda et al., 2020; Sweeney et al., 2022; Lin & Emanuel, 2022). However, in the nudged experiments differences in high cloud fraction are not related to precipitation or OLR anomalies. These results highlight that the simulated QBO teleconnections require tropical stratosphere-troposphere coupling and feedbacks.

One possible drawback of the nudging approach employed in this study is that the QBO winds have been nudged to the observations at all longitudes, in contrast to some studies that only nudge the zonal-mean values. While the QBO sets the zonal-mean temperature and wind, the local conditions of clouds, convection and temperature in the tropical UTLS are heavily influenced by feedbacks at the UTLS region involving the horizontal advection of clouds (Lin & Emanuel, 2022), static stability (Nie & Sobel, 2015), or upward wave propagation (Sakaeda et al., 2020; Holt et al., 2022). This means that if the QBO is linked to tropical convection in the UM through the interaction of upward wave propagation and high-clouds, or through large-scale zonal circulations, with the underlying SSTs, our nudging setup was not the appropriate to diagnose these mechanisms. Based on this hypothesis, the nudging at all longitudes of this study would weaken or even remove the influence of the lower troposphere on the local TTL and muting feedbacks potentially involving large-scale tropical circulations. However, further studies, with different types of nudging or with different models are required to test these hypotheses.

Open Research Section

The reanalysis, observational and CMIP6 data is publicly available (see references in main text). The simulation data will be made publicly available at the time of acceptance.

Acknowledgments

JLGF acknowledges support from an Oxford-Richards Scholarship.

References

Adler, R. F., Huffman, G. J., Chang, A., Ferraro, R., Xie, P.-P., Janowiak, J., … Nelkin, E. (2003). The version-2 global precipitation climatology project (GPCP) monthly precipitation analysis (1979–present). *Journal of hydrometeorology*, *4*(6), 1147–1167.

Allan, R. P. (2011). Combining satellite data and models to estimate cloud radiative effect at the surface and in the atmosphere. *Meteorological Applications*, *18*(3), 324–333.

Back, S.-Y., Han, J.-Y., & Son, S.-W. (2020). Modeling evidence of qbo-mjo connection: A case study. *Geophysical Research Letters*, *47*(20), e2020GL089480.

Baldwin, M., Gray, L., Dunkerton, T., Hamilton, K., Haynes, P., Randel, W., … others (2001). The quasi-biennial oscillation. *Reviews of Geophysics*, *39*(2), 179–229.

Bushell, A. C., Anstey, J. A., Butchart, N., Kawatani, Y., Osprey, S. M., Richter, J. H., … Yukimoto, S. (2020). Evaluation of the Quasi-Biennial Oscillation in global climate models for the SPARC QBO-initiative. *Quarterly Journal of the Royal Meteorological Society*, 1-31. Retrieved from `https://rmets.onlinelibrary.wiley.com/doi/abs/10.1002/qj.3765` doi: https://doi.org/10.1002/qj.3765

Byrne, M. P., & Zanna, L. (2020). Radiative effects of clouds and water vapor on an axisymmetric monsoon. *Journal of Climate*, *33*(20), 8789–8811.

Collimore, C. C., Martin, D. W., Hitchman, M. H., Huesmann, A., & Waliser, D. E. (2003). On the relationship between the QBO and tropical deep convection. *Journal of climate*, *16*(15), 2552–2568.

Davis, S. M., Liang, C. K., & Rosenlof, K. H. (2013). Interannual variability of tropical tropopause layer clouds. *Geophysical Research Letters*, *40*(11), 2862–2866.

Domeisen, D. I., Garfinkel, C. I., & Butler, A. H. (2019). The teleconnection of El Niño Southern Oscillation to the stratosphere. *Reviews of Geophysics*, *57*(1), 5–47.

García-Franco, J. L., Gray, L. J., Osprey, S., Chadwick, R., & Martin, Z. (2022). The tropical route of quasi-biennial oscillation (qbo) teleconnections in a climate model. *Weather and Climate Dynamics*, *3*(3), 825–844. doi: 10.5194/wcd-3-825-2022

Garfinkel, C. I., Gerber, E. P., Shamir, O., Rao, J., Jucker, M., White, I., & Paldor, N. (2022). A qbo cookbook: Sensitivity of the quasi-biennial oscillation to resolution, resolved waves, and parameterized gravity waves. *Journal of Advances in Modeling Earth Systems*, *14*(3), e2021MS002568.

Garfinkel, C. I., & Hartmann, D. L. (2011). The influence of the quasi-biennial oscillation on the troposphere in winter in a hierarchy of models. Part II: Perpetual winter WACCM runs. *Journal of the Atmospheric Sciences*, *68*(9), 2026–2041.

Geller, M. A., Zhou, T., & Yuan, W. (2016). The qbo, gravity waves forced by tropical convection, and enso. *Journal of Geophysical Research: Atmospheres*, *121*(15), 8886–8895.

Giorgetta, M. A., Bengtsson, L., & Arpe, K. (1999). An investigation of QBO signals in the east Asian and Indian monsoon in GCM experiments. *Climate dynamics*, *15*(6), 435–450.

Gray, L., Brown, M., Knight, J., Andrews, M., Lu, H., O'Reilly, C., & Anstey, J. (2020). Forecasting extreme stratospheric polar vortex events. *Nature communications*, *11*(1), 1–9.

Gray, L. J., Anstey, J. A., Kawatani, Y., Lu, H., Osprey, S., & Schenzinger, V. (2018). Surface impacts of the Quasi Biennial Oscillation. *Atmospheric Chemistry and Physics*, *18*(11), 8227–8247. doi: 10.5194/acp-18-8227-2018

Gray, W. M. (1984). Atlantic seasonal hurricane frequency. Part I: El Niño and 30 mb quasi-biennial oscillation influences. *Monthly Weather Review*, *112*(9), 1649–1668.

Gray, W. M., Sheaffer, J. D., & Knaff, J. A. (1992). Influence of the stratospheric QBO on ENSO variability. *Journal of the Meteorological Society of Japan. Ser. II*, *70*(5), 975–995.

Hartmann, D. L., & Berry, S. E. (2017). The balanced radiative effect of tropical anvil clouds. *Journal of Geophysical Research: Atmospheres*, *122*(9), 5003–5020.

Haynes, P., Hitchcock, P., Hitchman, M., Yoden, S., Hendon, H., Kiladis, G., ... Simpson, I. (2021). The influence of the stratosphere on the tropical troposphere. *Journal of the Meteorological Society of Japan. Ser. II*.

Hendon, H. H., & Abhik, S. (2018). Differences in vertical structure of the madden-julian oscillation associated with the quasi-biennial oscillation. *Geophysical Research Letters*, *45*(9), 4419–4428.

Hersbach, H., Bell, B., Berrisford, P., Hirahara, S., Horányi, A., Muñoz-Sabater, J., ... Thépaut, J.-N. (2020). The ERA5 global reanalysis. *Quarterly Journal of the Royal

Meteorological Society, *146*(730), 1999–2049. doi: 10.1002/qj.3803

Hitchman, M. H., Yoden, S., Haynes, P. H., Kumar, V., & Tegtmeier, S. (2021). An observational history of the direct influence of the stratospheric quasi-biennial oscillation on the tropical and subtropical upper troposphere and lower stratosphere. *Journal of the Meteorological Society of Japan. Ser. II*.

Holt, L. A., Lott, F., Garcia, R. R., Kiladis, G. N., Cheng, Y.-M., Anstey, J. A., ... others (2022). An evaluation of tropical waves and wave forcing of the qbo in the qboi models. *Quarterly Journal of the Royal Meteorological Society*, *148*(744), 1541–1567.

Hu, Z.-Z., Huang, B., Kinter, J. L., Wu, Z., & Kumar, A. (2012). Connection of the stratospheric QBO with global atmospheric general circulation and tropical SST. Part II: interdecadal variations. *Climate dynamics*, *38*(1), 25–43.

Kennedy, J. J., Rayner, N., Atkinson, C., & Killick, R. (2019). An ensemble data set of sea surface temperature change from 1850: The met office hadley centre hadsst. 4.0. 0.0 data set. *Journal of Geophysical Research: Atmospheres*, *124*(14), 7719–7763.

Kim, H., Caron, J. M., Richter, J. H., & Simpson, I. R. (2020). The lack of QBO-MJO Connection in CMIP6 Models. *Geophysical Research Letters*, *47*(11), e2020GL087295. (e2020GL087295 2020GL087295) doi: 10.1029/2020GL087295

Kim, H., Son, S.-W., & Yoo, C. (2020). Qbo modulation of the mjo-related precipitation in east asia. *Journal of Geophysical Research: Atmospheres*, *125*(4), e2019JD031929.

Kim, Y.-H., & Chun, H.-Y. (2015). Contributions of equatorial wave modes and parameterized gravity waves to the tropical qbo in hadgem2. *Journal of Geophysical Research: Atmospheres*, *120*(3), 1065–1090.

Lee, J. C. K., & Klingaman, N. P. (2018). The effect of the quasi-biennial oscillation on the Madden–Julian oscillation in the Met Office Unified Model Global Ocean Mixed Layer configuration. *Atmospheric Science Letters*, *19*(5), e816. doi: 10.1002/asl.816

Lee, J.-H., Kang, M.-J., & Chun, H.-Y. (2019). Differences in the tropical convective activities at the opposite phases of the quasi-biennial oscillation. *Asia-Pacific Journal of Atmospheric Sciences*, *55*(3), 317–336.

Liess, S., & Geller, M. A. (2012). On the relationship between qbo and distribution of tropical deep convection. *Journal of Geophysical Research: Atmospheres*, *117*(D3).

Lim, Y., & Son, S.-W. (2022). Qbo wind influence on mjo-induced temperature anomalies in the upper troposphere and lower stratosphere in an idealized model. *Journal of the Atmospheric Sciences*.

Lin, J., & Emanuel, K. (2022). Stratospheric modulation of the mjo through cirrus cloud feedbacks. *Journal of the Atmospheric Sciences*.

Martin, Z., Orbe, C., Wang, S., & Sobel, A. (2021a). The MJO–QBO Relationship in a GCM with Stratospheric Nudging. *Journal of Climate*, *34*(11), 4603–4624.

Martin, Z., Sobel, A., Butler, A., & Wang, S. (2021c). Variability in qbo temperature anomalies on annual and decadal time scales. *Journal of Climate*, *34*(2), 589–605.

Martin, Z., Son, S.-W., Butler, A., Hendon, H., Kim, H., Sobel, A., … Zhang, C. (2021b). The influence of the quasi-biennial oscillation on the madden–julian oscillation. *Nature Reviews Earth & Environment*, 1–13.

Martin, Z., Wang, S., Nie, J., & Sobel, A. (2019, 02). The Impact of the QBO on MJO Convection in Cloud-Resolving Simulations. *Journal of the Atmospheric Sciences*, *76*(3), 669-688.

Menary, M. B., Kuhlbrodt, T., Ridley, J., Andrews, M. B., Dimdore-Miles, O. B., Deshayes, J., … Xavier, P. (2018). Preindustrial control simulations with HadGEM3-GC3. 1 for CMIP6. *Journal of Advances in Modeling Earth Systems*, *10*(12), 3049–3075.

Nie, J., & Sobel, A. H. (2015). Responses of tropical deep convection to the QBO: Cloud-resolving simulations. *Journal of the Atmospheric Sciences*, *72*(9), 3625–3638.

Rao, J., Garfinkel, C. I., & White, I. P. (2020). How does the quasi-biennial oscillation affect the boreal winter tropospheric circulation in cmip5/6 models? *Journal of Climate*, *33*(20), 8975–8996.

Richter, J. H., Anstey, J. A., Butchart, N., Kawatani, Y., Meehl, G. A., Osprey, S., & Simpson, I. R. (2020). Progress in simulating the Quasi-Biennial Oscillation in CMIP models. *Journal of Geophysical Research: Atmospheres*, *125*(8), e2019JD032362. (e2019JD032362 10.1029/2019JD032362)

Sakaeda, N., Dias, J., & Kiladis, G. N. (2020). The unique characteristics and potential mechanisms of the mjo-qbo relationship. *Journal of Geophysical Research: Atmospheres*, *125*(17), e2020JD033196.

Schenzinger, V., Osprey, S., Gray, L., & Butchart, N. (2017). Defining metrics of the Quasi-Biennial oscillation in global climate models. *Geoscientific Model Development*, *10*(6).

Schirber, S. (2015). Influence of ENSO on the QBO: Results from an ensemble of idealized simulations. *Journal of Geophysical Research: Atmospheres*, *120*(3), 1109–1122.

Serva, F., Anstey, J. A., Bushell, A. C., Butchart, N., Cagnazzo, C., Gray, L., … Simpson, I. R. (2022). The impact of the QBO on the region of the tropical tropopause in QBOi models: present-day simulations. *Quaterly Journal of the Royal Meteorological Society*, *148*(745), 1945-1964. doi: https://doi.org/10.1002/qj.4287

Serva, F., Cagnazzo, C., Christiansen, B., & Yang, S. (2020). The influence of enso events on the stratospheric qbo in a multi-model ensemble. *Climate Dynamics*, *54*(3), 2561–2575.

Son, S.-W., Lim, Y., Yoo, C., Hendon, H. H., & Kim, J. (2017). Stratospheric control of the Madden–Julian oscillation. *Journal of Climate*, *30*(6), 1909–1922.

Storkey, D., Blaker, A. T., Mathiot, P., Megann, A., Aksenov, Y., Blockley, E. W., ... others (2018). UK Global Ocean GO6 and GO7: A traceable hierarchy of model resolutions. *Geoscientific Model Development*, *11*(8), 3187–3213.

Sun, L., Wang, H., & Liu, F. (2019). Combined effect of the qbo and enso on the mjo. *Atmospheric and Oceanic Science Letters*, *12*(3), 170–176.

Sweeney, A. J., Fu, Q., Pahlavan, H. A., & Haynes, P. (2022, aug). Seasonality of the QBO impact on equatorial clouds. *ESSOAR*. Retrieved from `https://doi.org/10.1002%2Fessoar.10512278.1` doi: 10.1002/essoar.10512278.1

Tegtmeier, S., Anstey, J., Davis, S., Ivanciu, I., Jia, Y., McPhee, D., & Pilch Kedzierski, R. (2020). Zonal Asymmetry of the QBO Temperature Signal in the Tropical Tropopause Region. *Geophysical Research Letters*, *47*(24), e2020GL089533. (e2020GL089533 2020GL089533) doi: https://doi.org/10.1029/2020GL089533

Telford, P., Braesicke, P., Morgenstern, O., & Pyle, J. (2008). Description and assessment of a nudged version of the new dynamics unified model. *Atmospheric Chemistry and Physics*, *8*(6), 1701–1712.

Trenberth, K. E. (1997). The definition of el nino. *Bulletin of the American Meteorological Society*, *78*(12), 2771–2778.

Tseng, H.-H., & Fu, Q. (2017). Temperature control of the variability of tropical tropopause layer cirrus clouds. *Journal of Geophysical Research: Atmospheres*, *122*(20), 11–062.

Walters, D., Boutle, I., Brooks, M., Melvin, T., Stratton, R., Vosper, S., ... Xavier, P. (2019). The Met Office Unified Model global atmosphere 7.0/7.1 and JULES global land 7.0 configurations. *Geoscientific Model Development*, *12*(5), 1909–1963.

Yoo, C., & Son, S.-W. (2016). Modulation of the boreal wintertime madden-julian oscillation by the stratospheric quasi-biennial oscillation. *Geophysical Research Letters*, *43*(3), 1392–1398.